ADJUSTABLE ELECTROMECHANICAL WEDGE BRAKES WITH REDUCED ENERGY CONSUMPTION

Vasily A. Ivanov

Bauman Moscow State Technical University
Robotics and Complex Automation Department
Moscow, Russia
vasiliya.ivanov@gmail.com

Beshah Ayalew

Clemson University
International Center for Automotive Research
4 Research Dr
Greenville, SC, USA
(864)283-7228
beshah@clemson.edu

ABSTRACT

An Electromechanical Wedge Brake (EWB) has an inherent self-reinforcing capability that translates into reduced actuation forces and subsequently into reduced energy requirements. However, to avoid jamming the brake, there is a need for a dedicated means of adjusting the effective wedge angle in order to modulate the braking forces and to accommodate changing pad friction conditions. Earlier prototypes had one actively controlled moveable wedge with a fixed wedge angle. In this paper, two new designs are considered and compared with the conventional EWB design. The first one uses pre-defined wedge shapes in a self-adjusting design with one movable wedge. The second uses an externally adjustable wedge and an actively movable wedge with similarly pre-defined wedge shapes. These designs can be employed to further reduce the required actuator forces beyond what is possible with the conventional design. The benefits of these self-adjusting and externally adjustable EWB designs are demonstrated using dynamic model simulations for a typical hard braking event.

1. INTRODUCTION

Electromechanical Wedge Brakes (EWBs) have recently received attention for implementing "brake-by-wire" solutions. Examples of research and development work on these brakes have been published by researchers at Siemens VDO [1-7], Mando Corporation [8] and Continental [9]. The findings largely confirm the fact that the use of a wedge in a mechanism of an electromechanical brake can reduce required actuation forces significantly [10-11]. As we will briefly review below, the extent of required actuator force amplification depends on a specific relation between the magnitude of the pad friction coefficient and the brake's wedge angle. With EWBs, this self-reinforcing nature is exploited to attempt to meet the increasing requirements on modern braking systems for reduced energy consumption, installation space, weight, cost and associated changes in system response and feel.

The main goal of the present work is to demonstrate that the magnitude of required actuator force (and energy) for EWBs can be reduced even more by measures that combine wedge shape design and controlled wedge adjustment. There is also an added benefit to adjust the brake wedge angle in a manner that accommodates changes in brake pad friction coefficient with wear, temperature, dirt inclusions, etc. In this paper, two proposed EWBs that employ pre-designed wedge shapes will be presented and analyzed.

The paper is organized as follows. Section 2 reviews the basic operation of a wedge brake, section 3 discusses the proposed adjustable EWBs, section 4 details the dynamic model adopted, section 5 presents the analyses of the designs, and section 6 gives the conclusions of the work.

2. BASIC OPERATION

The basic operating principles of a wedge brake mechanism are depicted in the schematic given in Fig. 1 below [1].
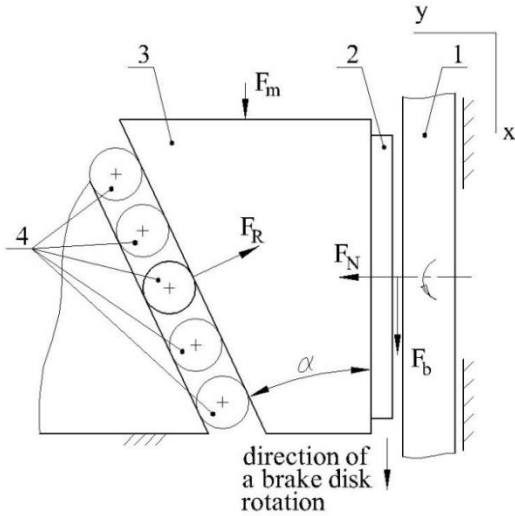
Fig. 1. Simplified model of conventional EWB [1]: 1 – brake disk; 2 - brake pad; 3 – active brake wedge; 4 – wedge abutment

In Fig. 1, the active brake wedge 3 has a surface inclined at an angle α and rests on rolling elements 4. Brake pad 2 is rigidly connected to wedge 3. The actuator, usually an electric motor acting through a screw drive mechanism, applies the force F_m on the wedge 3. Using the free body diagram of wedge 3, the relevant equations of statics are:

$$F_N - F_R \cos\alpha = 0 \tag{1}$$

$$F_b + F_m - F_R \sin\alpha = 0 \tag{2}$$

where F_b - braking force generated by friction in the contact zone between brake disk 1 and brake pad 2. Assuming a pad friction coefficient μ, the braking force is related to the normal force F_N through:

$$F_b = \mu F_N \tag{3}$$

Then, one can derive the following relationship between the actuator force and the braking force.

$$F_m = F_b \frac{\tan\alpha - \mu}{\mu} \tag{4}$$

Equation (4) gives the nominal actuator force F_m required for generating a desired braking force F_b. It also shows the self-reinforcing nature of the wedge mechanism that allows for using smaller magnitudes of actuator force to generate large braking forces. In the limit, the actuator force would be minimal (F_m approaches zero) for an arbitrary magnitude of braking force, as $\tan\alpha$ approaches μ. Conventional EWBs attempt to exploit this observation for saving actuation energy, weight, and cost, assuming that the friction coefficient is known to be roughly equivalent to tangent of the wedge angle. Due to

the changes of the pad friction coefficient over time (with wear, inclusions, temperature, etc.) there will be lost opportunities in continually maintaining this lower energy consumption benefit. In this work, it is considered that an adjustable and controlled EWB design may help exploit the self-reinforcing nature to further reduce the energy requirements and to maintain the benefits for extended periods despite changing pad friction coefficients.

3. ADJUSTABLE EWB APPROACH

In the present paper, we refer to an EWB with straight wedge surfaces and with an actively controlled wedge as a *conventional EWB*. We refer to an EWB that has specifically pre-defined wedge shapes that change the effective wedge angle as a function of the wedge position as a *self-adjusting EWB* (Fig. 2,3). And we call an EWB with pre-defined wedge surfaces both of which are movable, where one is actively controlled and one is externally adjustable, as an *externally adjustable EWB* (Fig. 4). Conventional EWBs and the motivation for self-adjusting EWBs have been previously mentioned in [1]. The externally adjustable EWB proposed here provides further possibilities for efficient wedge engagement. In the following, the workings of the self-adjusting and externally adjustable EWB are discussed in further detail.
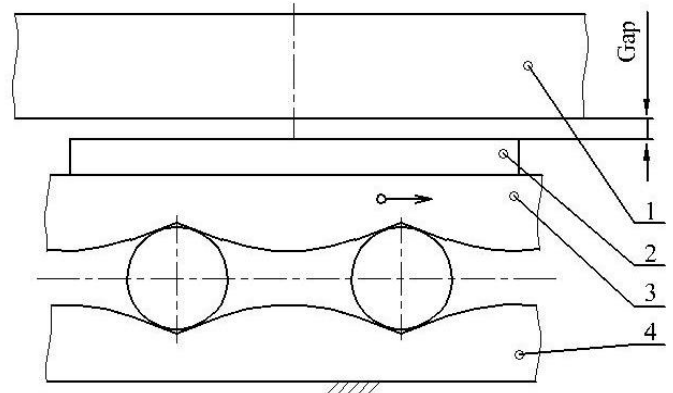
Fig. 2. Self-adjusting EWB: 1 – brake disk, 2 – brake pad, 3 – active wedge, 4 – fixed wedge

The proposed wedge surfaces of the self-adjusting EWB are predefined, and wedge 3 is movable, as shown in Figures 2-3. The braking process starts with displacement of wedge 3 to the right. After the gap between the brake pad and brake disk is eliminated with this movement, the wedges will be in contact with the rollers at points "a" (Fig. 3), with an effective wedge angle "a" and the brake is fully engaged around this point. The shape of the wedge surface has at least two distinct sections. While the gap is being eliminated, the shape gives a constant wedge angle between points 1 and "a" (Fig. 3). This angle is selected based on the most probable value of the friction coefficient. Beyond this point, the shape is such that the effective wedge angle decreases. This decrease allows for reducing the magnitude of the brake actuation force for the same level of braking force and friction coefficient (see

2   Copyright © 2011 by ASME

Equation 4). A well-designed control system would manage this reduction and possible reversal of the actuation force and prevent the brake from locking.
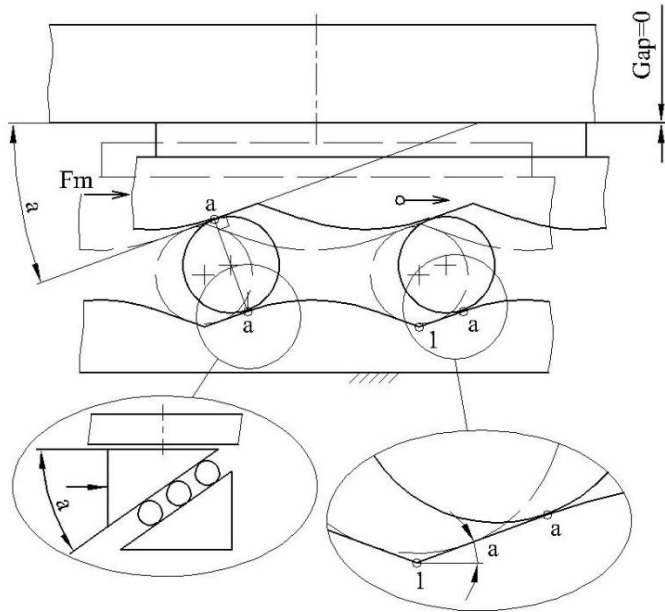
Fig. 3. Detail of self-adjusting EWB showing initial wedge angle "a" of the wedge shape

If an implementation of the EWB employs available real-time estimates of the pad friction coefficient (see Equation 13 below), the self-adjusting geometry can further be exploited to make adjustments based on the prevailing friction coefficient. For example, if the pad friction coefficient decreases below the tangent of the initial wedge angle, the active wedge can be pushed farther to have the brake engage beyond point "a" in Figure 3 (i. e., with reduced effective wedge angle). This will subsequently reduce the actuation force required to maintain engagement.

For the externally adjustable EWB, the two brake wedges are independently movable in the directions shown (Fig. 4). The active wedge 3, closest to the brake disk, is actuated in the direction parallel to the brake disk plane and for the present paper, wedge 4 is considered to be movable in the normal direction to the brake disk, even though other directions are also possible. In so doing, the effective wedge angle could be changed from, say "a" to "b". Wedge 4 has to go down leaving space for wedge 3 to go to the right even more and make way for the contact to move to point "b" (Fig. 4). Adjustments of the remote wedge can be performed while the vehicle is parked or when it is not braking assuming that the pad friction coefficient can be considered to not change very fast. Furthermore, the adjustment of wedge 4 can be done primarily passively, for example, by the use of a spring mechanism so as not to require an additional active actuator/motor.
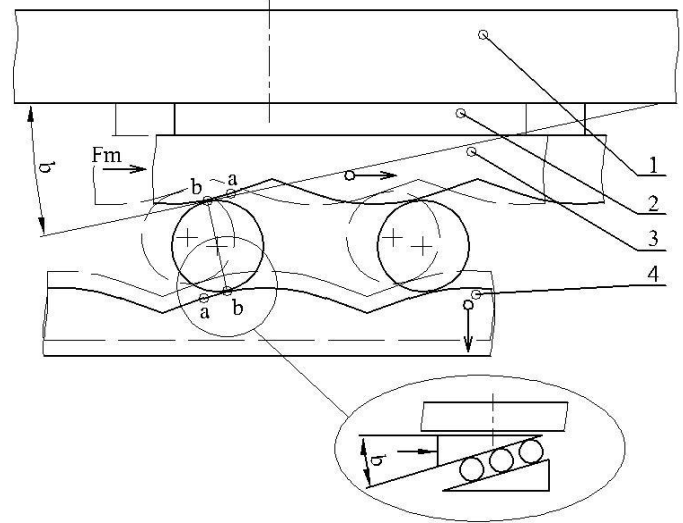
Fig. 4. Detail of an externally adjustable EWB: 1 – brake disk, 2 – brake pad, 3 – active wedge, 4 – externally adjustable wedge

Again, if pad friction estimates are available, the additional adjustment provisions in the externally adjustable EWB can be used to keep the value of wedge angle such that it corresponds to the friction coefficient ($\mu \approx tan\alpha$) at every point of the braking process to further minimize the actuation force/energy requirements.

4. DYNAMIC MODEL

In this section, a dynamic model of the wedge-brake system is adopted from [12] and customized to further analyze the workings of the EWB concepts. The schematic of the model is shown in Fig. 5. We consider that, for the cases analyzed, the effective wedge angle α changes with wedge displacement x_w. This models the shape of the active wedge for both the self-adjusting and externally adjusted EWBs. The actuator force F_m comes from a motor driving a roller screw mechanism of total equivalent translational mass m_A. This is connected to a wedge of mass m_w through stiffness K_A and damping coefficient D_A that take into account the compliance and damping in the drive. The roller screw has a lead L that transforms the motor torque T_M to the wedge actuation force F_m and the motor rotation ω_m to the actuator/screw translational displacement d_A. The brake caliper has a stiffness K_{cal} in the direction shown. Actuator force F_m acts with inclination angle β to the brake disk plane to account for mounting considerations. Assuming further that the angular differences between α and β are small, the equations of motion for the moving masses can be shown to be [12]:

$$m_A \ddot{d}_A = F_m - D_A\left(\dot{d}_A - \frac{\dot{x}_w}{\cos\alpha}\right) - K_A\left(d_A - \frac{x_w}{\cos\alpha}\right) - D_M \frac{2\pi}{L}\dot{d}_A \quad (5)$$

$$m_w \ddot{x}_w = \frac{1}{1+\tan^2\alpha}\left(\frac{1}{\cos\alpha}\left(D_A\left(\dot{d}_A - \frac{\dot{x}_w}{\cos\alpha}\right) + K_A\left(d_A - \frac{x_w}{\cos\alpha}\right)\right)\right) \quad (6)$$
$$+\left(\mu - \tan\alpha\right)K_{Cal}x_w\tan\alpha$$

3   Copyright © 2011 by ASME

where d_A - position of the equivalent translational mass m_A of a motor and roller screw mechanism, D_A - the viscous friction coefficient associated with this mechanism.

The drive motor is a high performance brushless DC motor whose armature electrical dynamics is given by [13]:

$$\frac{di_M}{dt} = -\frac{R_M}{L_M} i_M - \frac{k_M}{L_M} \omega_M + \frac{1}{L_M} u_M \tag{7}$$

$$\omega_M = \frac{2\pi}{L} \dot{d}_A \tag{8}$$

where L_M - inductance; i_m - motor current; R_M - resistance; u_m - motor input voltage. The motor torque is given by:

$$T_M = K_T i_M \tag{9}$$

where K_T - motor torque constant. Maxon motor EC 45 (136210) was used for the analysis in this work, and motor model parameters were taken from [14]. The actuator force is computed from the motor torque T_M using:

$$F_m = \frac{2\pi}{L} T_M \eta \tag{10}$$

where L - lead of screw mechanism [m], η - efficiency of screw mechanism.
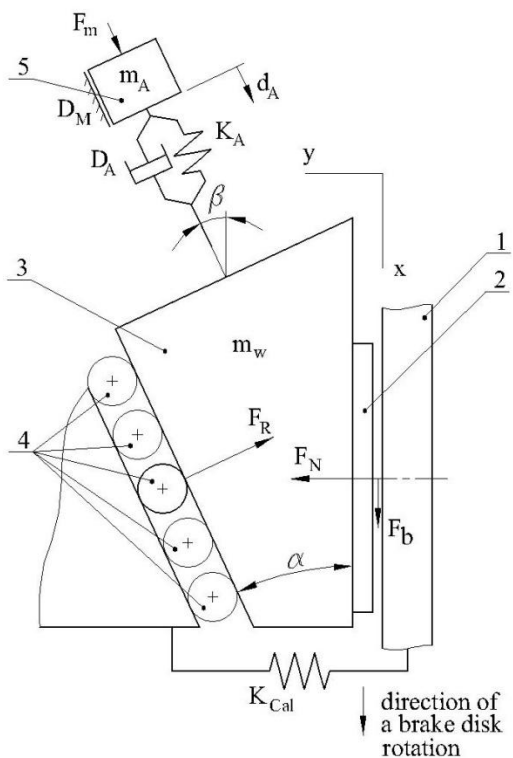
Fig. 5. Dynamic model of EWB (roughly represents top view): 1 –brake disk; 2 – brake pads; 3 – brake wedge; 4 – wedge abutment; 5 – floating brake caliper; 6 – translational mass of a roller screw mechanism

The above model of EWB was integrated within a larger model including the longitudinal quarter-car model of a vehicle and the dynamics of the braked-wheel [15]:

$$m\dot{V} = -F_g - F_r \tag{11}$$

$$J\dot{\omega} = RF_g - M_b \tag{12}$$

where, F_g is the tire/ground force, F_r is the motion resistance (aerodynamics, rolling resistance, etc), R is the wheel radius, and M_b is the applied braking torque.

A pad friction estimation scheme can also be set up. The normal force can be estimated by measuring the deformation of the brake caliper. And motor current sensor can be used to estimate the motor torque and hence the actuator force. Then, an estimate of the pad friction coefficient can be obtained by combining (3) and (4):

$$\mu = \tan\alpha - \frac{F_m}{F_N}. \tag{13}$$

For the investigations below, a standard cascaded controller is adopted from [12] for controlling the active wedge in all three types of EWBs. This controller is needed for generating the braking force in accordance with desired brake force that comes from driver.
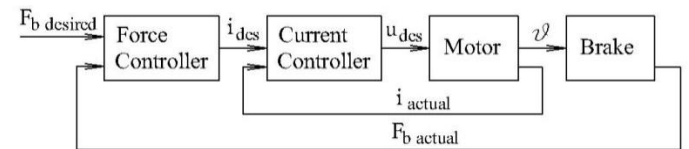
Fig. 6 shows a schematic of the controller. The cascade structure has the advantage that each loop can be tuned independently. The inner loop, the current controller, compares the desired and actual current, and outputs a demand voltage to the motor. The outer loop, the force controller, compares desired and actual braking forces and defines the desired motor current for the current controller. For the analysis in this paper, a PID controller was used for each control.
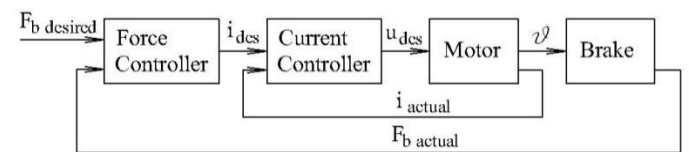
Fig. 6. Cascade control structure for the active wedge of EWBs

4   Copyright © 2011 by ASME

5. ANALYSIS WITH SIMULATED BRAKING TESTS

Assumptions on Wedge Angles/Shapes

The pre-designed wedge shapes considered for the simulation-based analysis of the three EWB designs are shown in Figure 7. The initial gap been pad and disk in all three EWBs is taken as *6 mm*. The value of pad friction coefficient μ for the present tests is assumed known and is equal to *0.2*. The bottom black solid line in Figure 7 is for the optimal wedge angle with this prevailing pad friction coefficient of *0.2*. The prevailing value is intentionally taken to be less than the design value in order to analyze how the different EWBs work under such conditions. The conventional EWB is designed for a probable pad friction coefficient value of *μ=0.35* [1], which corresponds to a nominal wedge angle of *19.6°* (*tan19.6° =0.35*).
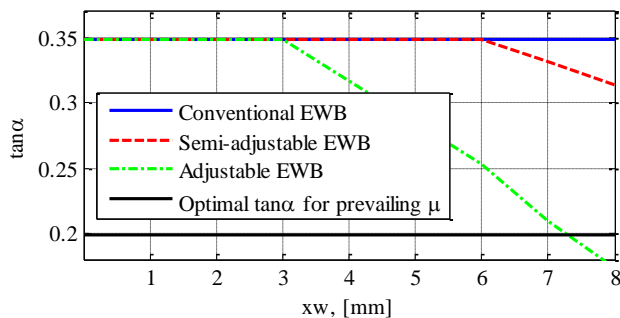
Fig. 7. Pre-designed effective wedge angles as a function of wedge position for the different EWBs

The wedge angle of a self-adjusting EWB has a slight bend after the 6mm wedge position corresponding to elimination of the gap. This pre-design considers the fact that the wedge brake goes farther than the 6mm gap only if considerable actuator forces that deform the brake caliper are applied. Reduction of wedge angle beyond this point is intended to reduce these actuator forces.

The wedge angle of the externally adjustable EWB is chosen to be approximately equal to the optimal wedge angle for the prevailing μ at extreme braking. In practice, the reduced wedge angle and forces imply that the brake caliper will be deformed less and the wedge travels less in this extreme case.

Simulated Braking Test Parameters

Braking tests were simulated for one wheel of a *1000 kg* vehicle stopping from an initial speed *33 m/s* (*120 km/h*) on a dry asphalt surface. Rolling and air resistance coefficients were taken as *0.01* and *0.4*, respectively. The frontal area of the vehicle was taken as *2 m²*. Fig. 8 shows the vehicle and wheel peripheral speeds for a hard braking event that commences at *2* seconds. A desired braking torque of *1300 Nm* is applied. This value of braking torque quickly locks the wheel within *0.7* seconds. Nearly identical baseline vehicle braking behaviors

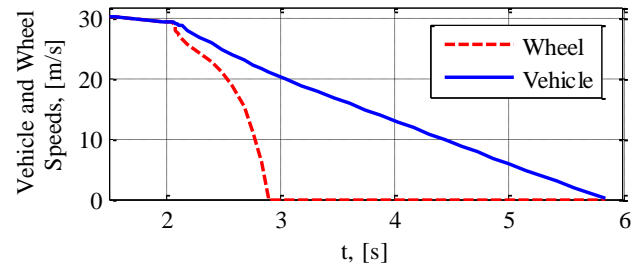are obtained by tuning the controllers for the three EWBs to the same gains.

Fig. 8. Wheel and vehicle speeds during braking with the three EWB designs

Analysis of the Performance of EWB Designs

Figure 9 shows the actual actuator and braking forces involved in the braking event described above. Braking forces reach the desired value *12 kN* in approximately *0.1* seconds after the actuator forces were applied. It can be seen that the actuator forces for the externally adjustable EWB are much smaller than the ones for the conventional and self-adjusting EWBs for approximately the same braking forces. The braking forces for the externally adjustable EWB rise slightly slower than the ones for the conventional and self-adjusting EWBs because the brake wedge of the externally adjustable EWB has a smaller effective wedge angle and needs to be pushed further to generate the same desired braking force. However, this difference in the dynamics of the EWBs is very small and had little effect on the braking distance of the vehicle under the tested conditions.
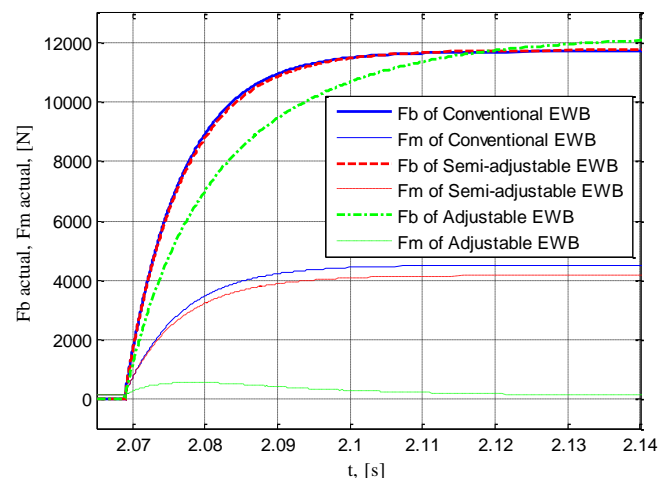
**Fig. 9. Evolution of the braking and actuator forces during braking event**

Fig. 10 illustrates the effective wedge angles of the three EWB designs during the same braking event. The wedge angle of the conventional EWB stays constant. For the self-adjusting EWB, there is a decrease in the effective wedge angle value at a specific time (after *2.07* second) corresponding to gap

5

Copyright © 2011 by ASME

elimination. As intended with the pre-designed shape shape (Figure 7), the effective wedge angle decreases beyond this point. For the externally adjustable EWB, there is an early decrease in wedge angle value (after *2.03* second), also as intended.
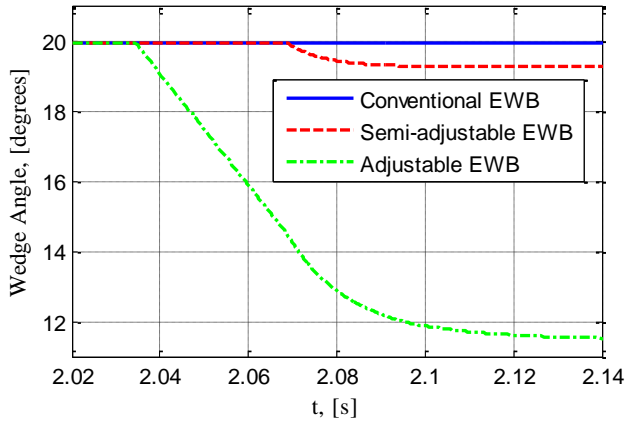
**Fig. 10. Effective wedge angle during braking event**

Fig. 11 shows the corresponding wedge position as a function of time. It can be seen that all wedges go *1-2 mm* further than necessary for gap elimination (*6 mm*) due to brake caliper deformation. As stated above, for the same braking force, it takes greater displacement for the externally adjustable EWB to deform the brake caliper than for the conventional and self-adjusting EWBs because the effective wedge angle of externally adjustable brake is less than that of the conventional and self-adjusting brakes (Figures 7, 10).
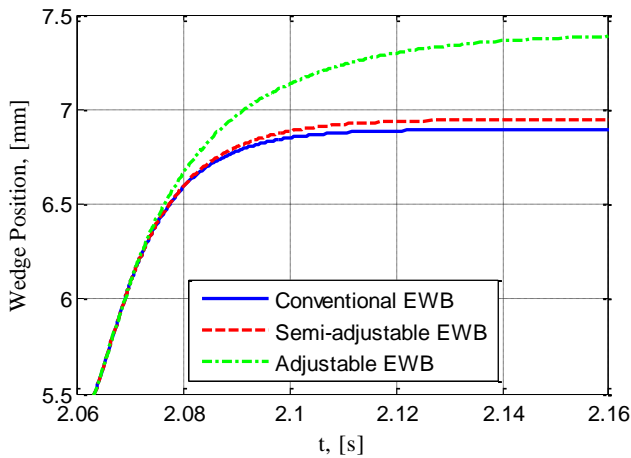
**Fig. 11. Evolution of wedge position during braking event**

Fig. 12, 13 show the motor torque and the motor control voltage, respectively, for the three EWBs during the same braking event. Obviously, the motor torque requirement for the externally adjustable EWB is considerably less than that for the self-adjusting and conventional EWBs. This feature of the externally adjustable EWB allows usage of compact motors

with lower torque/power rating that can lead to decrease of weight and energy consumption of the brake.
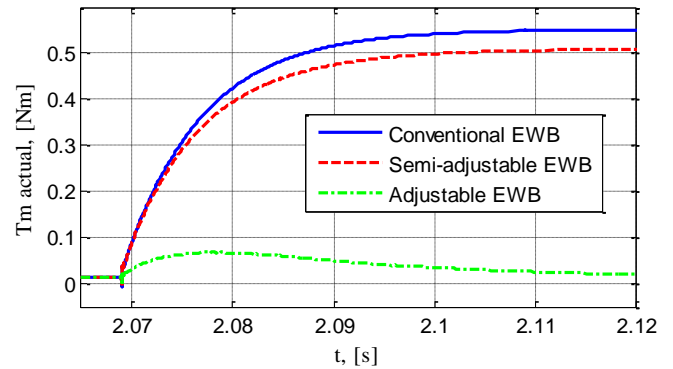
Fig. 12. Motor torque during the braking event

The initial voltage during brake pad gap elimination is constant (*2-2.069* second). Upon gap elimination and first engagement, there is a spike from the drastically changing stiffness on contact. After engagement the voltage drops to about *5* volts. This analysis suggests that it is possible to use existing *12*-volt electrical systems with a suitable up-converter or use a *24, 48*-volt or higher voltage system (as readily available with emerging EVs and HEVs) with a down-converter. In fact, with a different selection of the motor, it is possible to optimize the design and adjust the electrical requirements accordingly.
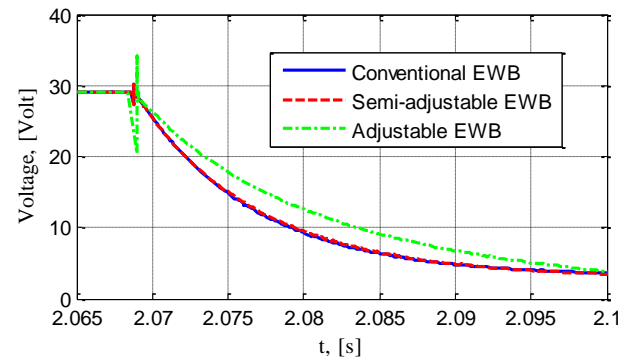
Fig. 13. Supplied motor voltage during the braking event

6. CONCLUSIONS AND OUTLOOK

The present paper presented and analyzed three electromechanical wedge brake (EWB) designs: a conventional, self-adjusting, and an externally adjustable EWB. The dynamic model of the EWB designs is simulated in a hard braking event. In this, all designs were tuned to achieve the same baseline stopping distances. Then, the three designs were analyzed by looking at the evolutions of the actuator and braking forces, the effective wedge angle, the wedge position, the motor torque and control voltage during the event. It is shown that while the self-adjusting EWB is an improvement over the conventional EWB, the externally adjustable EWB gives the best opportunity for minimizing torque requirements that translate to minimal

6   Copyright © 2011 by ASME

energy consumption. This also suggests that the externally adjustable EWB offers the possibility of downsizing of the brake system and saving packaging space, cost and improved dynamic feel.

Finally, it is remarked that the proposed adjustable EWBs can be made to work with existing electrical systems. These energy efficient designs make even more sense for incorporation into modern electric and hybrid vehicles (EVs and HEVs) that benefit from minimizing energy requirements for brake actuation/ boost systems.

DEFINITIONS, ACRONYMS, ABBREVIATIONS

α	wedge angle
β	angle between actuator force direction and brake disk plane
V	initial vehicle speed ($33\ m/s \approx 120\ km/h$)
m	vehicle weight ($1000\ kg$)
J	wheel inertia moment ($1.5\ kg\ast m^2$)
R	wheel radius ($0.313\ m$)
ω	wheel angle velocity
$M_{b\ desired}$	desired braking torque ($1300\ Nm$)
M_b	actual braking torque
M_g	ground torque
μ	friction coefficient between brake disk and pad (0.2)
F_R	reaction force
F_g	ground force
F_r	motion resistance
F_m	motor (actuator) force
F_b	actual braking force
$F_{b\ desired}$	desired braking force
F_N	normal force
i_M	actual motor current
$I_{M\ desired}$	desired motor current

T_M	motor torque
R_M	motor resistance ($0.143\ \Omega$)
L_M	motor inductance ($0.0565\ H$)
K_T	motor torque constant ($25\ast10^{-3}\ Nm/A$)
θ_M	motor angle
$\theta_{M\ desired}$	desired motor angle
ω_M	motor speed
u_M	actual motor voltage
$u_{M\ desired}$	desired motor voltage
m_w	mass of brake wedge ($0.7\ kg$)
x_w	wedge position in x_w direction
m_A	translational mass of a roller screw mechanism ($0.3\ kg$)
d_A	m_A position
K_A	actuator stiffness ($8\ast10^8\ N/m$)
D_A	actuator damping ($1\ast10^4\ Ns/m$)
D_M	constant of inside motor friction ($5\ast10^{-2}\ N$)
K_{Cal}	normal stiffness of brake caliper ($1.2\ast10^8\ N/m$)
L	screw mechanism lead ($0.5\ast10^{-3}\ m$)
η	screw mechanism efficiency (0.65)

REFERENCES

[1] H. Hartmann, M. Schautt, A. Pascucci, B. Gombert. (2002) "eBrake – the mechatronic wedge brake,". SAE Paper 2002-01-2582

[2] Johannes Dietrich, Bernd Gombert, Markus Grebenstein. (2001) US patent 6,318,513 "Electromechanical brake with self-energization"

[3] Lok Man Ho, Richard Roberts, Henry Hartmann, Bernd Gombert. (2006) "The Electronic Wedge Brake – EWB,". SAE Paper 2006-01-3196

[4] Ákos Semsey, Richard Roberts. (2006) "Simulation in the Development of the Electronic Wedge Brake,". SAE Paper 2006-01-0298

Copyright © 2011 by ASME

[5] Lok Man Ho, Richard Roberts, Henry Hartmann, Bernd Gombert. (2006) "The Electronic Wedge Brake – EWB,". SAE Paper 2006-01-3196

[6] Richard Roberts, Bernd Gombert, Henry Hartmann, Dittmar Lange & Martin Schautt. (2004) "Modelling and testing of the mechatronic wedge brake,". eStop Engineering GmbH & Co. K.G

[7] Henry Hartmann Bernd Gombert Richard Roberts & Martin Schautt. (2004) "A Progress Report on the Mechatronic Wedge Brake (eBrake). Practical Proof of the System Dynamics & Power Requirements,". eStop Engineering GmbH & Co. K.G

[8] Joo Gon Kim, Myoung June Kim, Jong Ki Kim, Ki-Han Noh, "Developing of Electronic Wedge Brake with Cross Wedge,". SAE Paper 2009-01-0856.

[9] (2011) "Continental Automotive", "Electronic Brake Systems": http://www.conti-online.com/generator/www/de/en/continental/automotive/themes/passenger_cars/chassis_safety/ebs/ebs_family/ebs_family_en.html, Retrieved May 5, 2011

[10] Roberts, Gombert, Hartmann, Lange, & Schautt. (2004) "Testing the Mechatronic Wedge Brake,". SAE Paper 2004-01-2766

[11] Ákos Semsey, Richard Roberts. (2006) "Simulation in the Development of the Electronic Wedge Brake,". SAE Paper 2006-01-0298

[12] J. Fox, R. Roberts, C. Baier-Welt, L. M. Ho, L. Lacraru, B. Gombert. (2007) "Modeling and Control of a Single Motor Electronic Wedge Brake,". SAE Paper 2007-01-0866

[13] Roberts, Schautt, Hartmann, & Gombert. (2003) "Modeling and Validation of the Mechatronic Wedge Brake,". SAE Paper 2003-01-3331

[14] (2011) "DC Motors, Brushless and Small DC Motors, Servo Motor, Gearheads, Motion Control" http://www.maxonmotorusa.com/, Retrieved May 5, 2011

[15] Bosch Gmbh, BOSCH Automotive Handbook (2000), 5th edition

8